GEOMATICS AND ENVIRONMENTAL ENGINEERING • Volume 18 • Number 5 • 2024

https://doi.org/10.7494/geom.2024.18.5.5

Taffy Elian[1], Naufal Setiawan[2]

Variability and Correlation among SST, Chlorophyll-a Levels, ENSO, and Pelagic Fishing in Southern Part of Madura Strait, Indonesia, Based on Landsat 9 OLI/TIRS Imagery

Abstract: Indonesia's marine resources are abundant, with fishing being a primary focus. The effective management of these resources requires an understanding of the factors that influence them, such as sea surface temperature (SST), El Niño-Southern Oscillation (ENSO) as indicated by the Southern Oscillation Index (SOI), and chlorophyll-a levels as food sources. This research aimed to elucidate the relationships among those factors at Madura Strait by utilizing their characteristics in response to the electromagnetic wavelengths that can be found Landsat 9 OLI/TIRS satellite images.

This research utilized the satellite's Thermal Infrared Sensor (or Band 10) (10.6–11.19 μm) to obtain the SST levels as well as the OceanColor 2 (OC2) algorithm to process Band 2 (0.45–0.51 μm) and Band 3 (0.53–0.59 μm) in order to obtain the chlorophyll-a levels. The results were the mean values of the SST (21.42 and 20.60°C) and the chlorophyll-a levels (0.77 and 0.87 mg/m^3) from the periods of June through August 2022 and December 2022 through February 2023, respectively. Furthermore, a correlation test and *t*-test were conducted, which indicated that the chlorophyll-a levels were contradictory with the SST, SOI, and total pelagic fish catches (which were in alignment). The *t*-test results only indicated significant correlations between the SST and chlorophyll-a levels (–0.806) and between the SST and SOI (0.732), while the other correlation was not significant.

Keywords: Landsat 9, sea surface temperature (SST), chlorophyll-a, Southern Oscillation Index (SOI), small pelagic fish, El Niño-Southern Oscillation (ENSO)

Received: March 27, 2024; accepted: August 21, 2024

[1] Universitas Pembangunan Nasional "Veteran," Faculty of Mineral Technology, Geomatics Engineering, Yogyakarta, Indonesia, https://orcid.org/0009-0009-3311-7700

[2] Universitas Pembangunan Nasional "Veteran," Faculty of Mineral Technology, Geomatics Engineering, Yogyakarta, Indonesia, email: naufal.setiawan@upnyk.ac.id (corresponding author), https://orcid.org/0000-0002-2350-4477

1. Introduction

Indonesia is one of the largest archipelagic countries in the world, with a vast ocean area of up to 3.25 million km^2 [1] that holds many resources (including fisheries). One of the commodities with a high economic value is the small pelagic fish that live near the ocean surface. To optimize the utilization of existing resources, science and continuous technological innovation can be utilized to observe oceanographic conditions.

The productivity of marine resource utilization (such as fishing) is influenced by oceanographic conditions (such as the ideal water temperature for small pelagic fish); seasonal changes and any climatic events can also affect this. The distribution of small pelagic fish can be determined by analyzing the spatial distribution of their food sources. One indicator of food sources is chlorophyll-a levels – the pigment of phytoplankton [2, 3]; therefore, the distribution small pelagic fish could be inferred from the distribution of the surface chlorophyll-a [4–7].

The distribution of chlorophyll-a levels is closely related to the oceanographic conditions of a water body [8]. Phytoplankton need an ideal environment, such as exposure to sunlight and a suitable sea surface temperature (SST). The influence of the SST on phytoplankton growth will indirectly affect the chlorophyll-a concentration in waters [9]. This phenomenon could also be found in research by [10], which proved variations in sea surface temperatures due to the west and east monsoons. This research also found that chlorophyll-a levels were quite high on the coast and became lower offshore; this was caused by the presence of river runoff that carried higher levels of organic matter. Thus, chlorophyll-a levels are higher in coastal rather than offshore areas [11].

The SST not only impacts the availability of food sources for small pelagic fish; it also influences the distribution of small pelagic fish, as it has been shown to affect fish growth [12, 13]. Changes in the SST can be attributed to seasonal fluctuations (including the west and east monsoon seasons [10, 14]) as well as other factors such as variations in sea level pressure – specifically, the El Niño-Southern Oscillation (ENSO) [15], which impacts the SST and wind direction in accordance with Charles's law. The ENSO phenomenon can be identified by the Southern Oscillation Index (SOI), which indicates the occurrence of the La Niña and El Niño phenomena (as reported by the Australian Bureau of Meteorology) [16].

Research by [17] examined the variability of the SST, salinity, and rainfall data during the ENSO phenomenon in Madura Strait within a 12-year span (from 2010 through 2021). The study revealed that the SST exhibited a significant increase during La Niña events, whereas it exhibited a corresponding decrease during El Niño events. This positive correlation could also be observed in the research that was conducted by [18] in the Malacca Strait (which analyzed data spanning from 1982 through 2014) as well as in research that was conducted in the Banda Sea [19].

The researchers that were mentioned above leveraged remote-sensing methodologies in order to conduct their observations. Chlorophyll-a levels and the SST

could be derived from the object's response to electromagnetic waves, whether they were reflected, emitted, or scattered back [20] with remote sensing; thus, there was no need for direct contact with the object [21]. The SST and chlorophyll-a levels could be detected by using satellite images, since the satellite sensor captured the amounts of the reflectance (chlorophyll-a reflects visible green light and absorbs blue and orange light waves) [22]. In our research, chlorophyll-a-level extraction was carried out using the OceanColor 2 (OC2) algorithm involving Band 2 (0.45–0.51 μm) and Band 3 (0.53–0.59 μm), while the SST levels were obtained from the Thermal Infrared Sensors (TIRS) (or Band 10) (10.60–11.19 μm).

According to [23], water bodies are classified as open sea waters, coastal waters, and inland waters. According to [24, 25], the OC2 and OC3 algorithms are more suitable for use in coastal and inland waters when compared to other available algorithms. The OC2 algorithm is a quartic polynomial algorithm that utilizes reflectance values from the blue and green channels [26, 27]. The blue and green spectrum is used to retrieve chlorophyll-a levels by detecting the blue-wave-absorption peak considering the strong signal-to-noise ratio (SNR) at this wavelength [26, 28, 29]. The authors of [11] proved that, when using the OC2 algorithm, chlorophyll-a-level-extraction processes were achievable using Landsat 8 OLI/TIRS. Aside from this, the newer Landsat satellite (Landsat 9 OLI/TIRS satellite imagery) has a resolution of 30 meters for each pixel for the multispectral as well as the TIRS band according to Google Earth Engine data catalog (this is a higher resolution than other satellite images such as MODIS Aqua/Terra, SNPP-VIIRS, and MERIS).

Moreover, the ENSO phenomenon that is indicated by the SOI would correlate to the SST, chlorophyll-a levels, and small pelagic fish catches. This could be found since SOI and the SST would affect the chlorophyll-a levels (and, thus, the small pelagic fish's food sources). Landsat 9 OLI/TIRS images are expected to be highly detailed since it has a better resolution than other satellite images.

As far as we know, no research has been conducted by using Landsat 9 OLI/TIRS satellite imagery to acquire SSTs and chlorophyll-a concentrations. This research shows the performance of the Landsat 9 OLI/TIRS satellite imagery to extract SST and chlorophyll-a levels, which will be tested with other variables such as the SOI index and the total number of pelagic fish catches in Madura Strait in order to determine the correlation among the variables using the Pearson product-moment correlation test and the *t*-test for validating our hypothesis.

2. State of Problems

While utilizing marine resources, a lack of information about oceanographic conditions is one of the significant challenges; these include information about ENSO's correlation with chlorophyll-a levels, the SST, and their impacts on fisheries. ENSO (which affects SST variability) is primarily caused by the differences in sea level pressure that, in turn, affect the growth and distribution of

phytoplankton (whose chlorophyll-a pigments are a crucial component of small pelagic fish's food sources). Furthermore, this affects the distribution and abundance of fish populations. ENSO can be identified by SOI, which can lead to a decrease in chlorophyll-a levels due to changes in the ocean's circulation and temperature. This decrease in chlorophyll-a levels can have negative impacts on fisheries, as fish populations rely on these nutrient-rich waters for survival.

In addition, there is a research gap that has not applied the Landsat 9 OLI/TIRS satellite images to estimate the chlorophyll-a levels and SSTs; hence, it is should be filled in order to support decision-making processes and sustainable practices. Moreover, this creates a knowledge gap by limiting our understanding of Landsat 9 OLI/TIRS's ability to obtain the spatial and temporal variability of chlorophyll-a levels and SSTs in response to ENSO events. Furthermore, the lack of a high-resolution data set on chlorophyll-a levels and SSTs in the study area during ENSO events hinders our ability to accurately model and predict the effect that ENSO has on fisheries and aquaculture.

3. Material and Methods

3.1. Study Area

The study area of this research was located in the southern part of Madura Strait which can be seen in Figure 1.

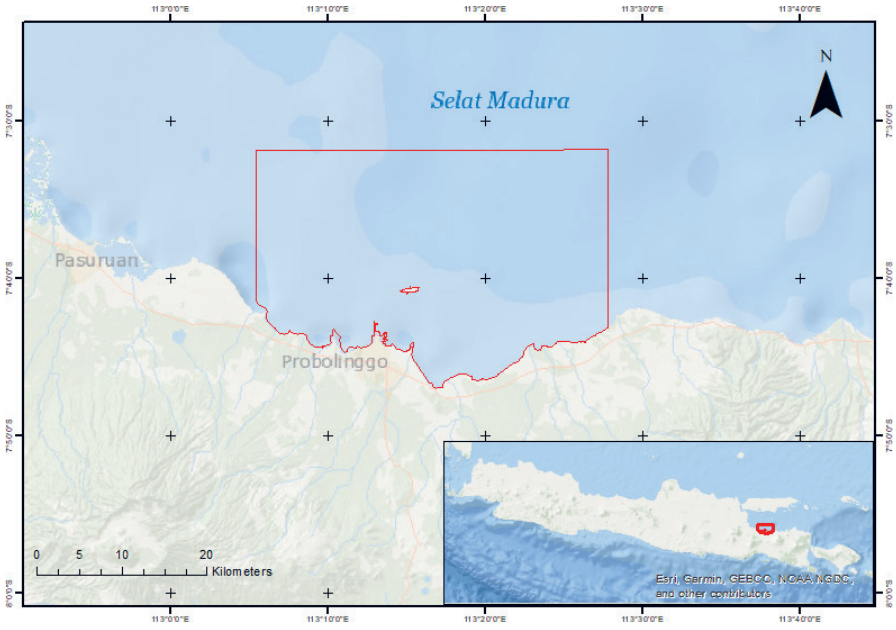

Fig. 1. Study area

Madura Strait is included in the Fisheries Management Area of Indonesia Number 712. Madura Strait (which lies on the north side of Probolinggo) is the primary source of income for fishermen, as it provides valuable resources. Fish distribution is needed to maximize the utilization of these resources by using satellite images to collect information on the SST and chlorophyll-a levels. This location was chosen because of the primary data availability in the form of Landsat 9 OLI/TIRS satellite imagery and the availability of secondary data on the numbers of small pelagic fish catches in 2022 and 2023.

3.2. Materials

This research was conducted from June 2022 through February 2023, with ten images of Landsat 9 OLI/TIRS Collection 2 Level 1 TOA over Madura Strait being acquired. The images from December 4, 2022, and February 6, 2023, were not used due to the cloud coverage on these days; images with higher cloud coverage cannot provide any visual nor non-visual information. For example, clouds are captured in the multispectral sensors, which means that the results would affected by the clouds' existence.

While the satellite images were derived from the Google Earth Engine (GEE) data catalogue, the small-pelagic-fish-catch data was obtained through a request from the Department of Agriculture, Food Security, and Fisheries (DPKPP) of Probolinggo, and the SOI index was downloaded from the Australian Bureau of Meteorology website (www.bom.gov.au). The fish-catch data was in the form of a table, consisting of Probolinggo's monthly fish and other catches (in tons). The SOI data was downloaded in a monthly form; it was given in positive numbers (which indicated the occurrence of La Niña) and negative numbers (indicating the presence of El Niño).

In contrast, both data sets can be seen in Table 1. We utilized Google Earth Engine (GEE) (to process the satellite images), Microsoft Excel (to process the statistics), and QGIS software (to create the maps).

Table 1. SOI and numbers of small pelagic fish catches

Date	SOI	Small pelagic fish catches [t]
June 2022	21.20	24.30
July 2022	8.70	14.00
August 2022	9.10	5.60
December 2022	20.00	9.60
January 2023	11.80	12.00
February 2023	10.50	11.40

Sources: small pelagic fish catches from Department of Agriculture, Food Security, and Fisheries (DPKPP) of Probolinggo (dpkpp.probolinggokab.go.id); SOI can be downloaded from Australian Government Bureau of Meteorology (bom.gov.au)

3.3. Methods

SST Value Retrieval

As a cloud-computing platform, utilizing Google Earth Engine eased the processing due to its faster processing time, as it did not require us to first download the images (in addition, some processes were passed over; i.e., radiometric and atmospheric corrections). Band 10 (10.6–11.19 μm) from the Thermal Infrared Sensors (TIRS) was used to retrieve the SST values. Since Landsat 9 OLI/TIRS Collection 2 Tier 1 Top of Atmosphere (TOA) Reflectance data sets already have TOA brightness temperatures shown in kelvins. In this research, this data was converted to degrees Celsius by using Equation (1):

$$\text{Celsius} = \text{Kelvin} - 273 \tag{1}$$

where:

Celsius – temperature in degrees Celsius,
Kelvin – temperature in kelvins.

Chlorophyll-a Level Retrieval

Based on [26], OceanColor 2 (OC2) is a quartic polynomial that is used to retrieve chlorophyll-a levels based on the remote sensing reflectance values (R_{rs}) from Band 2 (0.45–0.51 μm) and Band 3 (0.53–0.59 μm). Reflectance (R_{rs}) is the number of electromagnetic waves that are reflected by an objects' responses. The algorithm's statistical and graphical results were considered to be superior to other formulations that were equated along its simple and reversible functional form. Band 2 (0.45–0.51 μm) and Band 3 (0.53–0.59 μm), which are the blue- and green-color spectrums, respectively, were used to retrieve the chlorophyll-a levels by detecting the blue-wave absorption peak, considering the strong signal-to-noise ratio (SNR) at this wavelength [26, 28, 29]. To retrieve the chlorophyll-a levels from the Landsat 9 OLI/TIRS images, Equation (2) was used:

$$Chla = 10^{a0+a1\cdot R+a2\cdot R^2+a3\cdot R^3} + a4 \tag{2}$$

where:

$Chla$ – chlorophyll-a levels [mg/m^3],
$a0 = 0.341$,
$a1 = -3.001$,
$a2 = 2.811$,
$a3 = -2.041$,
$a4 = 0.0400$,

$$R_{rs} = \log\frac{R_{rs}490}{R_{rs}555} = \log\frac{R_{rs}\,band\,2}{R_{rs}\,band\,3}.$$

Validations

Validation is a crucial step during research; without this procedure, research findings may be flawed or misleading, thus leading to incorrect conclusions. Validation is done using the Pearson product-moment correlation test to obtain any correlation and the *t*-test for hypothesis validation. Before processing the statistical data with the Pearson product-moment correlation test, the SST values, chlorophyll-a levels, SOI, and total fish catches were sorted into monthly data (like the other data); for instance, SOI and the total fish-catch data. To obtain the correlation between each variable pairing, the correlation test was done using Equation (3):

$$r_{XY} = \frac{n\sum XY - \sum X \sum Y}{\sqrt{\left\{n\sum X^2 - \left(\sum X\right)^2\right\}\left\{n\sum Y^2 - \left(\sum Y\right)^2\right\}}} \tag{3}$$

where:

X – first variable,
Y – second variable,
r_{XY} – correlation coefficient,
n – number of samples.

The data that had been correlation-tested was processed further for the *t*-test by comparing the calculated results and the *t*-value based on the significance and the number of samples. This test was carried out by choosing a two-tailed test with a 0.2 significance level test (due to the limitations of the satellite image availability of only 10 images); a lower significance level (which means more precision) could have been achieved by processing more images. The *t*-test was done by processing the data using the *t*-test formula that is shown in Equation (4):

$$t = \frac{r\sqrt{n-2}}{\sqrt{1-r^2}} \tag{4}$$

where:

t – calculation result,
r – second variable,
n – number of sample.

4. Results and Discussion

All of the processed Landsat 9 OLI/TIRS images produced SST values and chlorophyll-a levels. To get the maximum results that reflected the actual conditions, the cloud-masking process was performed in order to delete some parts of the images that were covered by clouds. During this process, some parts of the cloudy

areas were not removed, as the algorithm has its limitations. Figure 2 shows the parts where the cloud-masking algorithm did not run perfectly when processing the Landsat 9 OLI/TIRS image from June 11, 2022. These unmasked areas affected the statistical results of the SST values and chlorophyll-a levels.

Fig. 2. Unmasked cloud-covered areas

4.1. Sea Surface Temperature

After Landsat 9's Band 10 (10.6–11.19 μm) images were processed, they showed the results of the SST variability along the southern part of Madura Strait. The results of the SST-extraction process from June through August 2022 are shown in Figure 3. The SSTs are shown with a green-to-red color range, which started from 17.5 to 26°C; this indicated lower sea surface temperatures in green and higher sea surface temperatures in red (as shown in Figure 3). As can be seen in Figure 3, the images from June 11, 2022, showed that the western side of the map was colored green; these were areas that were not masked as cloudy areas during the cloud-masking process. In another image from August 14, 2022, some areas around the masked areas were unmasked due to the limits of the cloud-masking process.

Figure 3 shows that there was a decrease in the SST, as the images had turned from yellowish to green on August 30, 2022. During this period, the monthly mean SSTs for June, July, and August 2022 were 22.56, 21.61, and 20.08°C, respectively (the average was 21.42°C). Further details about the statistical values of the SSTs can be seen in Table 2.

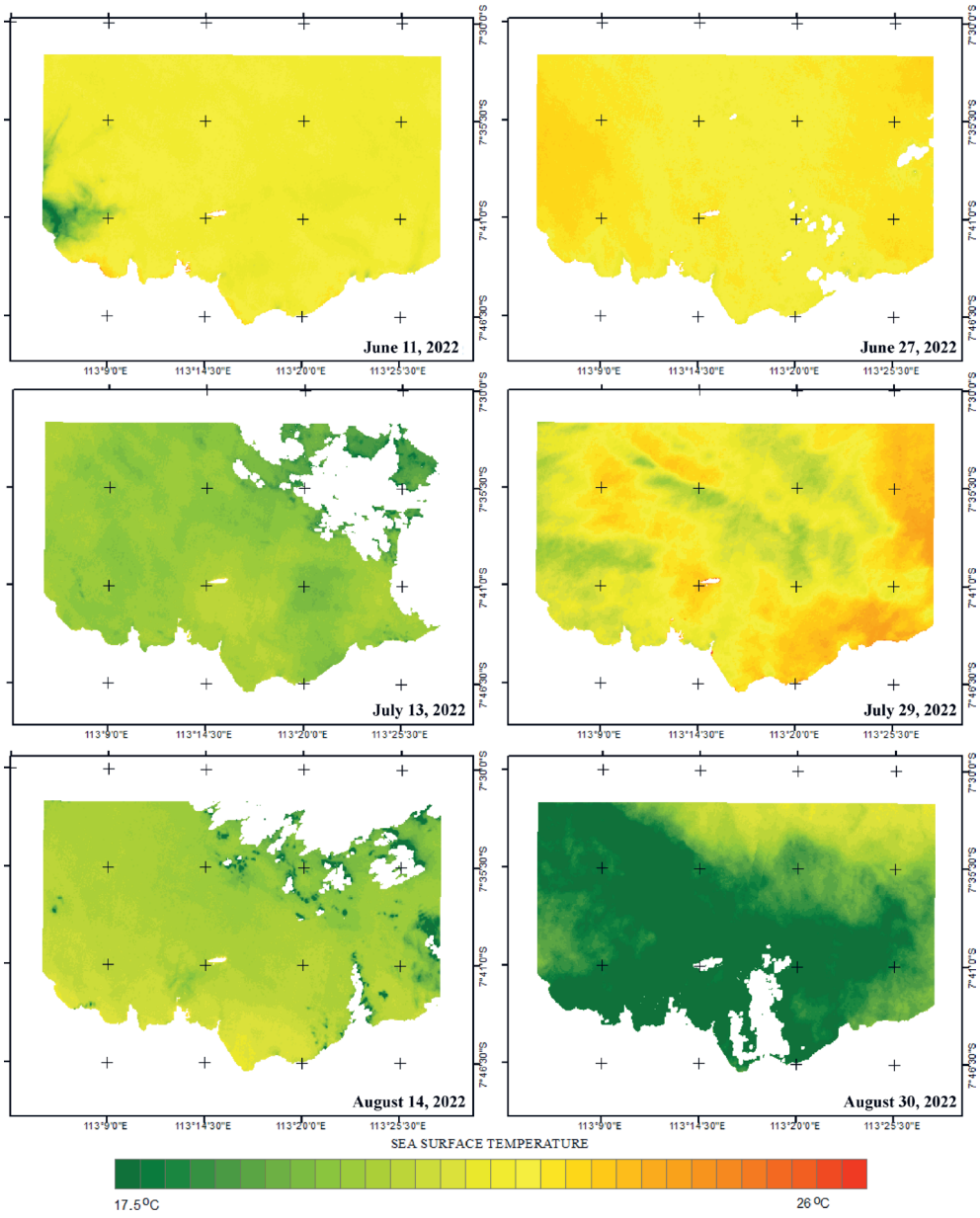

Fig. 3. SST-variability map from June through August 2022

Based on the statistical values in Table 2, there was a decreasing mean value of the SSTs during this period, while the lowest temperature could be found on August 30, 2022 (19.15°C). Additionally, there were some extreme values of the minimum temperature of August 14, 2022. This phenomenon occurred due to

a cloud-masking process that was not optimal. The highest SST mean was acquired from the images from June 27, 2022 (22.75°C), while the lowest was acquired from the images from August 30, 2022 (19.15°C).

Table 2. Sea surface temperatures from June through August 2022 [°C]

Date	Mean	Min	Max
June 11, 2022	22.36	17.86	25.18
June 27, 2022	22.75	21.24	24.46
July 13, 2022	20.73	17.01	24.10
July 29, 2022	22.49	20.61	28.90
August 14, 2022	21.02	−4.77	24.20
August 30, 2022	19.15	16.49	22.16

The second period (from December 2022 through February 2023) had a lower average SST of 21.42°C. Also, the monthly mean value of the SSTs decreased to its lowest on January 21, 2023 (17.18°C). During this period, the highest mean of the SST could be found on December 20, 2022 (22.73°C). There were also extreme differences among the minimum temperatures that occurred due to the limitations of the cloud-masking process.

Figure 4 shows the variability of the SSTs where the images turned from yellowish to solid green on January 21, 2023 (with the lowest mean value of the SST of this period). As could be seen on the images from August 14, 2022, January 5, 2023, and February 22, 2023, there was a phenomenon where the offshore area had higher temperatures than the coastal area did. This could have occurred due to any carried biomaterial from the waterways or river runoffs [10].

The data in Table 3 below shows that the SST mean on December 20, 2022, was 22.73°C; then, it dropped to 17.18°C on January 21, 2023, as the lowest mean (as previously mentioned). However, the lowest minimum SST was acquired on January 5, 2023, due to the limitations of the cloud-masking process. Visually, the lowest minimum SST could be seen around the removed parts of the image.

Table 3. Sea surface temperatures from December 2022 through February 2023 [°C]

Date	Mean	Min	Max
December 20, 2022	22.73	21.75	26.67
January 5, 2023	21.05	13.21	25.46
January 21, 2023	17.18	14.62	20.61
February 22, 2023	19.94	15.30	24.30

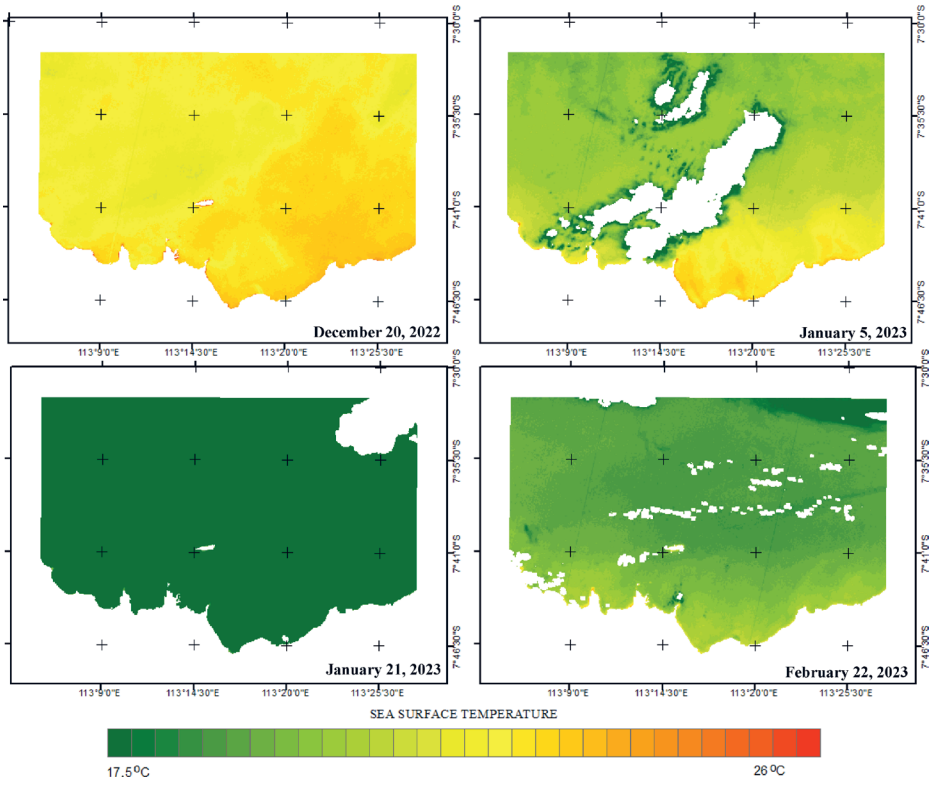

Fig. 4. SST-variability map from December 2022 through February 2023

Furthermore, the average SST mean of Madura Strait was grouped into a monthly period for the Pearson product-moment correlation test with other variables such as chlorophyll-a levels, SOI, and the number of fish catches (as shown in Table 4). By comparing both periods, the December 2022 through February 2023 period had lower averages than the other period did; this phenomenon could also be seen in the research by [10, 15]. By comparing this to the data in Table 1, the SSTs unidirectionally corresponded with the decreased SOI values.

Table 4. Sea surface temperatures of Madura Strait [°C]

Date	Mean
June 2022	22.56
July 2022	21.61
August 2022	20.08
December 2022	22.73
January 2023	19.12
February 2023	19.94

4.2. Chlorophyll-a Levels

The chlorophyll-a levels were acquired by processing the Landsat 9 OLI/TIRS images using the OceanColor 2 (OC2) algorithm, which utilized the reflectance values from the blue and green bands [26, 27]. Figure 5 shows that the coastal area had higher chlorophyll-a levels (purple color), while the lower levels were offshore (turquoise color). These phenomena could have been caused by the carried nutrients from the surrounding waterways or river runoffs [10].

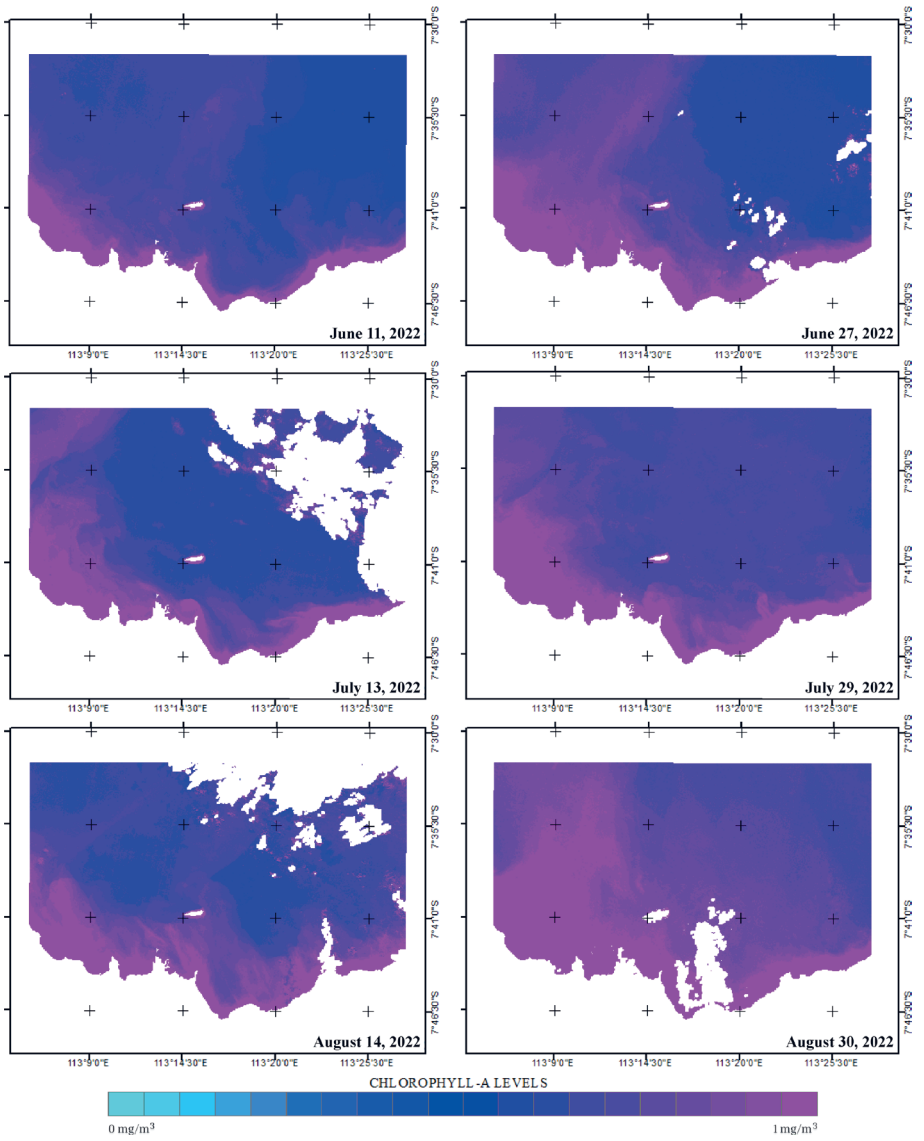

Fig. 5. Chlorophyll-a-level-variability map from June through August 2022

However, there were still higher chlorophyll-a levels around the cloud-masked areas; these higher chlorophyll-a levels were skewed by the clouds that were supposedly not masked. Since Bands 2 and 3 are multispectral, any visible unmasked clouds were processed by the OceanColor 2 algorithm.

Figure 5 shows increases in the mean chlorophyll-a levels from June 11, 2022, through their peak on August 30, 2022; this is indicated by the large amount of purple that replaced the bluish color. Furthermore, the images from June 11, 2022, and July 13, 2022, appeared to show more parts with lower chlorophyll-a levels (indicated by the blue color) than the other images that were supported by the data in Table 5; this shows chlorophyll-a levels of 0.7 mg/m^3 in the June 11 image, followed by the image from July 13, 2022 (0.75 mg/m^3).

The highest chlorophyll-a levels from June through August 2022 were shown in the image from July 29, 2022 (0.8 mg/m^3). Although the averages of each image ranged from 0.70 to 0.87 mg/m^3, the maximum values of each image ranged from 2.01 to 3.01 mg/m^3. While the average chlorophyll-a levels ranged 0.70–0.87 mg/m^3, the maximum values were dramatically higher (up to 3 mg/m^3); this was affected by the presence of unmasked clouds.

Table 5. Chlorophyll-a levels from June through August 2022 [mg/m^3]

Date	Mean	Min	Max
June 11, 2022	0.70	0.55	2.48
June 27, 2022	0.76	0.55	2.51
July 13, 2022	0.75	0.59	2.54
July 29, 2022	0.80	0.63	3.01
August 14, 2022	0.76	0.37	2.87
August 30, 2022	0.87	0.63	2.01

During the second period, there were higher chlorophyll-a levels than there were in the previous period (as is indicated by the purplish color in Figure 6). Also, the coastal areas had higher chlorophyll-a levels; these levels decreased further out from the shore. Although there was a void of the image from the beginning of February, increasing chlorophyll-a levels can be seen in Table 6. Increases of chlorophyll-a levels were discovered from December 20, 2022, through their peak on January 5, 2023; this was similar to the increases from January 21, 2022, through February 22, 2023. The highest mean of the chlorophyll-a levels was indicated by the image from January 5, 2023 (0.98 mg/m^3), while the lowest mean level during this period could be found on December 20, 2022 (0.81 mg/m^3).

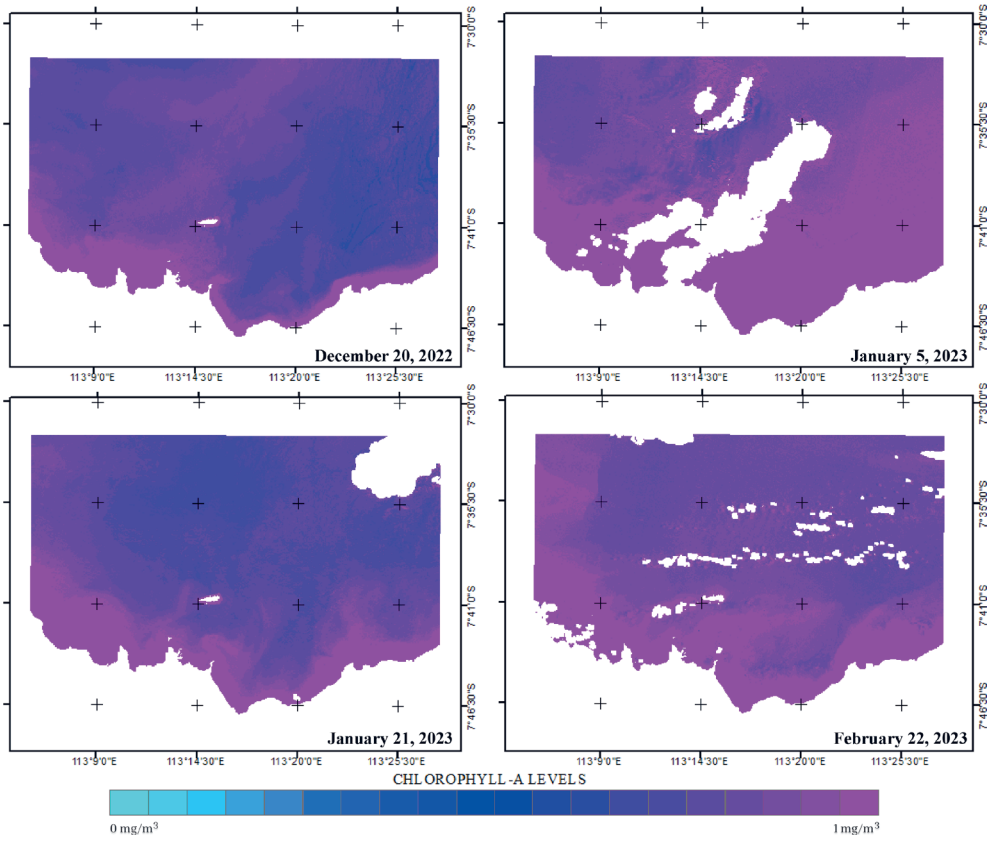

Fig. 6. Chlorophyll-a-level-variability map from December 2022 through February 2023

Table 6. Chlorophyll-a levels from December 2022 through February 2023 [mg/m^3]

Date	Mean	Min	Max
December 20, 2022	0.81	0.60	3.29
January 5, 2023	0.98	0.47	3.28
January 21, 2023	0.82	0.63	2.53
February 22, 2023	0.91	0.47	3.93

Furthermore, the average chlorophyll-a levels were grouped into monthly data (as shown in Table 7). The second period (which occurred from December 2022 through February 2023) had a higher average than in the previous period, with differences of up to 0.11 mg/m^3. The highest average was achieved in February 2023, followed by January 2023 (with a difference of 0.01 mg/m^3). These results were supported by the results of research from 2010 to 2019 [4].

The research by [30] also proved that the highest chlorophyll-a levels were achieved in the northwest monsoon around the month of January; this could have been caused by the change of the cooler-rich nutrients from below (a so-called upwelling) [31]. In addition, this showed that the chlorophyll-a levels and the SSTs were in opposition.

Table 7. Chlorophyll-a levels [mg/m^3]

Date	Mean
June 2022	0.73
July 2022	0.77
August 2022	0.82
December 2022	0.81
January 2023	0.90
February 2023	0.91

4.3. Validations

A Pearson product-moment correlation was carried out as the first step of the validation process in this research. This process was performed in order to obtain information about the directions and strengths of the relationships among the SSTs, chlorophyll-a levels, total pelagic fish catches, and SOI. The results of this correlation test are shown in Table 8.

Table 8. Pearson product-moment correlation test results

Variable	*r*
Sea surface temperature – Chlorophyll-a levels	−0.806
Sea surface temperature – Southern Oscillation Index	0.732
Sea surface temperature – Total pelagic fish catches	0.479
Chlorophyll-a levels – Southern Oscillation Index	−0.469
Chlorophyll-a levels – Total pelagic fish catches	−0.554
Southern Oscillation Index – Total pelagic fish catches	0.564

Each negative value indicates a pairing that had an opposite correlation, such as the correlation of the chlorophyll-a levels to each of the other variables (SST, SOI, and total pelagic fish catches); the remaining correlations were unidirectional. The results showed that there were warmer SSTs during La Niña (which was unidirectional with SOI [15, 17]) and that the chlorophyll-a levels decreased [32]. The positive correlation between SST and SOI was in line with Charles's law, which states that temperature has a unidirectional correlation with pressure. The highest correlation between SST and SOI could be found during the period from December 2022 through February 2023, with a correlation coefficient (r) of 0.94, while the period from June through August 2022 had a correlation coefficient (r) of 0.77.

Although the SST and chlorophyll-a levels had an opposite correlation, they were the highest at 0.806. Despite this, an anomalous phenomenon was captured by the image on June 27, 2022, where there was an increase in the SST as compared to the image on June 11, 2022; however, this was not accompanied by a decrease in the chlorophyll-a concentration. The same phenomenon could also be found in the image on February 22, 2023, where there was a significant increase in the chlorophyll-a concentration (up to 0.09 mg/m^3) despite experiencing an increase of up to 2.76°C in temperature. Similar phenomena were also found in the research that was conducted in the Makassar Strait [11], where the chlorophyll-a levels and the SST were not found to be in opposition.

Since some species of small pelagic fish respond to ENSO [33], the correlation between the SST and small pelagic fish catches was found to be 0.479; this indicated a moderate relationship between SPL and the quantity of small pelagic fish catches, meaning that the relationship between the SST and the number of pelagic fish catches was unidirectional. However, SST only affected the amount of small pelagic fish catches by 22.9441%, with the remainder being influenced by other factors such as salinity conditions, seasons, and other factors (such as the fishing intensity of fishermen).

At the same time, the lowest correlation was between chlorophyll-a levels and SOI (−0.469); this indicated that ENSO did not have a strong correlation with the chlorophyll-a levels [34]. The chlorophyll-a level, which reflects the amount of chlorophyll-a on the surface) is one indicator of food sources for small pelagic fish [2, 3]; this can be used as inferred information about the distribution of small pelagic fish [4–7].

Despite the fact that chlorophyll-a is a food source for small pelagic fish, this study found a strong but inversed correlation between chlorophyll-a concentrations and the catch quantities of small pelagic fish (with a correlation coefficient of –0.554). This inverse relationship could also be observed in a study that was conducted in the waters of Rembang Regency [35]. Last, a strong and direct correlation between SOI and the number of small pelagic fish catches could be found, with a correlation coefficient (r) of 0.564. Furthermore, the correlation test results were processed further by using a t-test to determine whether the hypothesis was accepted or rejected.

Table 9. Partial *t*-test results

Variable	*t*
SST – Chlorophyll-a levels	−2.72336
SST – SOI	2.14882
SST – Small pelagic fish catches	1.09135
Chlorophyll-a levels – SOI	−1.06205
Chlorophyll-a levels – Small pelagic fish catches	−1.3309
SOI – Small pelagic fish catches	1.36599

The final step of the validation process of this research was the *t*-test, which was carried out by processing the previous test results (*r*) from the Pearson product-moment correlation test. This test also classified the results based on the relationships between each pair of variables. In this research, the test was carried out by testing the calculated *t* value in Table 9 with the *t* critical value with a significance level of 0.05 (one-tailed); thus, the *t* value was 2.131847. Based on these values, there were only two correlations between pairs of variables (the SST – chlorophyll-a levels, and the correlation between SST and SOI); this showed significant correlations between these variable pairings. This issue may have arisen due to the limited amount of data, which may have not adequately captured the relationships between these variable pairings and tended to have biases [36].

5. Conclusions

It can be concluded that Landsat 9 OLI/TIRS images can used to retrieve the SST and chlorophyll-a levels of Madura Strait by utilizing the TIRS band (B10) while using the OceanColor 2 algorithm to retrieve the chlorophyll-a levels. The results showed that only two significant correlations could be found based on the result of the two-tailed test with a 0.2 significance level *t*-test, which were the correlation between the SST and chlorophyll-a levels (−0.806, with a significance level of −2.72336) and the correlation between the SST and SOI (0.732, with a significance level of 2.14882). The negative correlation between the SST and chlorophyll-a levels could have occurred when the surface waters were cold; in such a scenario, it is easier for deeper water to rise to the surface, thus bringing more nutrients to sunlit areas where phytoplankton can feed on them [37]. Therefore, the SST and chlorophyll-a levels had an opposite correlation; this supported the research that was performed by [30].

Further research should be conducted in order to acquire more information about the causal relationship between those variables with more satellite images in order to achieve maximum reliability. This research aimed to serve as a reference for utilizing Landsat 9 OLI/TIRS for acquiring SST and chlorophyll-a levels.

Funding

This research received no specific grant from any funding agency in the public, commercial, or not-for-profit sectors.

CRediT Author Contribution

T. E.: writing, study conception and design, material preparation, data collection, methodology, visualization, and analysis.

N. S.: writing and supervision.

Declaration of Competing Interest

The authors declare that they have no known competing financial interests or personal relationships that could have appeared to influence the work that is reported in this paper.

Data Availability

The data that supported this research (such as SOI) was derived from http://www.bom.gov.au/climate/enso/soi/. While the Landsat 9 OLI/TIRS images were retrieved from the Google Earth Engine data set, the small-pelagic-fish-catch data is available on request. The code that was used to process the Landsat 9 OLI/TIRS images can be found at the following link: https://code.earthengine.google.com/0bfc50e775840c4bfb2484036056fae1.

Use of Generative AI and AI-assisted Technologies

No generative AI or AI-assisted technologies were employed in the preparation of this manuscript.

References

[1] Pratama O.: *Konservasi Perairan Sebagai Upaya menjaga Potensi Kelautan dan Perikanan Indonesia*. 2020. https://kkp.go.id/djprl/artikel/21045-konservasi-perairan-sebagai-upaya-menjaga-potensi-kelautan-dan-perikanan-indonesia [access: 3.12.2023].

[2] Zhang C., Han M.I.N.: *Mapping chlorophyll-a concentration in Laizhou Bay using Landsat 8 OLI data*. [in:] Mynett A. (ed.), *Proceedings of the 36th IAHR World Congress 2015: Deltas of the Future and What Happens Upstream: The Hague, The Netherlands, 28 June–3 July 2015*, International Assn for Hydro-Environment Engineering and Research, 2015, pp. 12–17.

[3] Ma'mun A., Priatna A., Amri K., Nurdin E.: *Hubungan Antara Kondisi Oseanografi dan Distribusi Spasial Ikan Pelagis di Wilayah Pengelolaan Perikanan Negara Republik Indonesia (WPP NRI) 712 Laut Jawa*. Jurnal Penelitian Perikanan Indonesia, vol. 25(1), 2019, pp. 1–14.

[4] Atmadipoera A.S., Nugroho D., Jaya I., Akhir M.F.: *Simulated seasonal oceanographic changes and their implication for the small pelagic fisheries in the Java Sea, Indonesia*. Marine Environmental Research, vol. 188, 2023, 106012. https://doi.org/10.1016/j.marenvres.2023.106012.

[5] Chen H.H., Tang R., Zhang H.R., Yu Y., Wang Y.: *Investigating the relationship between sea surface chlorophyll and major features of the South China Sea with satellite information*. JoVE (Journal of Visualized Experiments), vol. 13(160), 2020, e61172. https://doi.org/10.3791/61172.

[6] Muskananfola M.R., Wirasatriya A.*: Spatio-temporal distribution of chlorophyll-a concentration, sea surface temperature and wind speed using aqua-modis satellite imagery over the Savu Sea, Indonesia*. Remote Sensing Applications: Society and Environment, vol. 22, 2021, 100483. https://doi.org/10.1016/j.rsase.2021.100483.

[7] Shen C., Yan Y., Zhao H., Pan J.T., Devlin A.: *Influence of monsoonal winds on chlorophyll-α distribution in the Beibu Gulf*. Plos One, vol. 13(1), 2018, e0191051. https://doi.org/10.1371/journal.pone.0191051.

[8] Syetiawan A.: *Penentuan Zona Potensi Penangkapan Ikan Berdasarkan Sebaran Klorofil-a*. Jurnal Ilmiah Geomatika, vol. 21(2), 2015, pp. 131–136.

[9] Sidik A., Agussalim A., Ridho M.R.: *Akurasi nilai konsentrasi klorofil-a dan suhu permukaan laut menggunakan data penginderaan jauh di Perairan Pulau Alanggantang Taman Nasional Sembilang*. Maspari Journal: Marine Science Research, vol. 7(2), 2015, pp. 25–32.

[10] Kurniawati F., Sanjoto T.B., Juhadi: *Pendugaan Zona Potensi Penangkapan Ikan Pelagis Kecil di Perairan Laut Jawa pada Musim Barat dan Musim Timur dengan Menggunakan Citra Aqua-MODIS*. Geo Image, vol. 4(2), 2015, pp. 9–19.

[11] Daming W.S., Amran M.A., Muhiddin A.H., Tambaru R.: *Spatial-Temporal Distribution of Chlorophyll-a in Southern Part of the Makassar Strait*. Jurnal Ilmu Kelautan SPERMONDE, vol. 4(1), 2018, pp. 42–46. https://doi.org/10.20956/jiks.v4i1.3804.

[12] Yuniarti A., Maslukah L., Helmi M.: *Studi variabilitas suhu permukaan laut berdasarkan citra satelit aqua MODIS tahun 2007–2011 di Perairan Selat Bali*. Journal of Oceanography, vol. 2(4), 2013, pp. 416–421. https://ejournal3.undip.ac.id/index.php/joce/article/view/4588.

[13] Brosset P., Fromentin J.M., Van Beveren E., Lloret J., Marques V., Basilone G., Bonanno A., Carpi P., Donato F., Čikeš Keč V., De Felice A., Ferreri R., Gašparević D., Giráldez A., Gücü A., Iglesias M., Leonori I., Palomera I., Somarakis S., Tičina V., Torres P., Ventero A., Zorica B., Ménard F., Saraux C.: *Spatio-temporal patterns and environmental controls of small pelagic fish body condition from contrasted Mediterranean areas*. Progress in Oceanography, vol. 151, 2017, pp. 149–162. https://doi.org/10.1016/j.pocean.2016.12.002.

[14] Rahadian L.D., Khan A.M., Dewanti L.P., Apriliani I.M.*: Analisis Sebaran Suhu Permukaan Laut pada Musim Barat dan Musim Timur Terhadap Produksi Hasil Tangkapan Ikan Lemuru (Sardinella lemuru) Di Perairan Selat Bali*. Jurnal Perikanan Kelautan, vol. 10(2), 2019, pp. 28–34.

[15] Wirasatriya A., Prasetyawan I.B., Triyono C.D., Maslukah L.: *Effect of ENSO on the variability of SST and Chlorophyll-a in Java Sea*. IOP Conference Series: Earth and Environmental Science, vol. 116(1), 2018, 012063. https://doi.org/10.1088/1755-1315/116/1/012063.

[16] Wang M., Guo J.R., Song J., Fu Y.Z., Sui W.Y., Li Y.Q., Zhu Z.M., Li S., Li L.L., Guo X.F., Zuo W.T.: *The correlation between ENSO events and sea surface temperature anomaly in the Bohai Sea and Yellow Sea*. Regional Studies in Marine Science, vol. 35, 2020, 101228. https://doi.org/10.1016/j.rsma.2020.101228.

[17] Toding J.E., Widagdo S., Bintoro R.S.: *Variabilitas Temperatur Permukaan Laut, Salinitas, dan, Curah Hujan Pada Periode El Niño-Southern Oscillation (Enso) di Perairan Selat Madura*. Jurnal Riset Kelautan Tropis (Journal of Tropical Marine Research) (J-Tropimar), vol. 4(1), 2022, pp. 52–66. https://doi.org/10.30649/jrkt.v4i1.60.

[18] Isa N.S., Akhir M.F., Kok P.H., Daud N.R., Khalil I., Roseli N.H.: *Spatial and temporal variability of sea surface temperature during El-Niño Southern Oscillation and Indian Ocean Dipole in the Strait of Malacca and Andaman Sea*. Regional Studies in Marine Science, vol. 39, 2020, 101402. https://doi.org/10.1016/j.rsma.2020.101402.

[19] Nababan B., Sihombing E.G.B., Panjaitan J.P.: *Variabilitas suhu permukaan laut (SPL) dan konsentrasi klorofil-a di Samudera Hindia bagian Timur Laut sebelah barat Sumatera*. Jurnal Teknologi Perikanan dan Kelautan, vol. 12(2), 2021, pp. 143–159. https://doi.org/10.24319/jtpk.12.143-159.

[20] Fery J., Haeruddin, Faizin N., Aminah S., Fanteri Aji D.S., Kristianta F.X.: *The use of remote sensing in mining prospecting in Situbondo, East Java, Indonesia*. AIP Conference Proceedings, vol. 2278(1), 2020, 020007. https://doi.org/10.1063/5.0014683.

[21] Lillesand T., Kiefer R.W., Chipman J.: *Remote Sensing and Image Interpretation*. 7th ed. John Wiley & Sons, 2015.

[22] Milne B.F., Toker Y., Rubio A., Nielsen S.B.: *Unraveling the intrinsic color of chlorophyll*. Angewandte Chemie International Edition, vol. 54(7), 2015, pp. 2170–2173. https://doi.org/10.1002/anie.201410899.

[23] Morel A., Prieur L.: *Analysis of variations in ocean color 1*. Limnology and Oceanography, vol. 22(4), 1977, pp. 709–722. https://doi.org/10.4319/lo.1977.22.4.0709.

[24] O'Reilly J.E., Maritorena S., O'Brien M.C., Siegel D.A., Toole D., Menzies D., Smith R.C., Mueller J.L., Mitchell B.G., Kahru M., Chavez R.P., Strutton P., Cota G.F., Hooker S.B., McClain C.R., Carder K.L., Mueller-Karger F., Harding L., Magnusion A., ..., Phinney D.: *SeaWiFS Postlaunch Calibration*

and Validation Analyses, Part 3. SeaWiFS Postlaunch Technical Report Series, vol. 11, NASA Center for AeroSpace Information, Goddard Space Flight Center, Greenbelt, Maryland 2000.

[25] Poddar S., Chacko N., Swain D.: *Estimation of chlorophyll-a in the northern coastal Bay of Bengal using Landsat-8 OLI and Sentinel-2 MSI sensors*. Frontiers in Marine Science, vol. 6, 2019, 598. https://doi.org/10.3389/fmars.2019.00598.

[26] O'Reilly J.E., Maritorena S., Mitchell B.G., Siegel D.A., Carder K.L., Garver S.A., Kahru M., McClain C.: *Ocean color chlorophyll algorithms for SeaWiFS*. Journal of Geophysical Research: Oceans, vol. 103(C11), 1998, pp. 24937–24953. https://doi.org/10.1029/98JC02160.

[27] Dierssen H.M.: *Perspectives on empirical approaches for ocean color remote sensing of chlorophyll in a changing climate*. Proceedings of the National Academy of Sciences, vol. 107(40), 2010, pp. 17073–17078. https://doi.org/10.1073/pnas.0913800107.

[28] Gordon H.R., Brown O.B., Evans R.H., Brown J.W., Smith R.C., Baker K.S., Clark D.K.: *A semianalytic radiance model of ocean color*. Journal of Geophysical Research: Atmospheres, vol. 93(D9), 1988, pp. 10909–10924. https://doi.org/10.1029/JD093iD09p10909.

[29] Zeng C., Xu H., Fischer A.M.: *Chlorophyll-a estimation around the Antarctica peninsula using satellite algorithms: hints from field water leaving reflectance*. Sensors, vol. 16(12), 2016, 2075. https://doi.org/10.3390/s16122075.

[30] Handoko E., Hayati N., Syariz M., Hanansyah M.: *Analysis of chlorophyll-a variability in the Eastern Indonesian waters using Sentinel-3 OLCI from 2020–2021*. Forum Geografi, vol. 38(1), 2024, pp. 74–82. https://doi.org/10.23917/forgeo.v38i1.2361.

[31] Hendiarti N., Suwarso E.A., Amri K., Andiastuti R., Sachoemar S.I., Wahyono I.B.: *Seasonal variation of pelagic fish catch around Java*. Oceanography, vol. 18(4), 2005, pp. 112–123. https://doi.org/10.5670/oceanog.2005.12.

[32] Wijaya A., Zakiyah U.M.I., Sambah A.B., Setyohadi D.: *Spatio-temporal variability of temperature and chlorophyll-a concentration of sea surface in Bali Strait, Indonesia*. Biodiversitas Journal of Biological Diversity, vol. 21(11), 2020, pp. 5283–5290. https://doi.org/10.13057/biodiv/d211132.

[33] Puspasari R., Rahmawati P.F., Prianto E.: *The effect of ENSO (El Nino Southern Oscillation) phenomenon on fishing season of small pelagic fishes in Indonesia waters*. IOP Conference Series: Earth and Environmental Science, vol. 934(1), 2021, 012018. https://doi.org/10.1088/1755-1315/934/1/012018.

[34] Maisyarah S., Wirasatriya A., Marwoto J., Subardjo P., Prasetyawan I.B.: *The effect of the ENSO on the variability of SST and chlorophyll-a in the South China Sea*. IOP Conference Series: Earth and Environmental Science, vol. 246(1), 2019, 012027. https://doi.org/10.1088/1755-1315/246/1/012027.

[35] Dwiyanti A., Maslukah L., Rifai A.: *Pengaruh Suhu Permukaan Laut (SPL) dan Klorofil-A Terhadap Hasil Tangkapan Ikan Layang (Decapterus macrosoma) di Perairan Kabupaten Rembang, Jawa Tengah*. Indonesian Journal of Oceanography, vol. 4(4), 2023, pp. 109–120. https://doi.org/10.14710/ijoce.v4i4.15708.

[36] Ahmad K., Conci N., Boato G., De Natale F.G.: *USED: A large-scale social event detection dataset*. [in:] *MMSys '16: Proceedings of the 7th International Conference on Multimedia Systems: Klagenfurt, Austria, May 10–13, 2016*, Association for Computing Machinery, New York 2016, pp. 1–6. https://doi.org/10.1145/2910017.2910624.

[37] NASA Earth Observatory: *Sea Surface Temperature & Chlorophyll*. https://earthobservatory.nasa.gov/global-maps/MYD28M/MY1DMM_CHLORA [access: 22.06.2024].